Impact of the StatCom on the Power System Feasibility Region Boundary

H.R. Carvajal-Peréz, C. R. Fuerte-Esquivel

Abstract— **A feasibility region of a power system is defined by all operating points that can be reached by continuous variation of parameters without causing system's instability. The boundary of this region is composed by bifurcation surfaces. When surfaces associated to Hopf bifurcations intersect each other, emerges a 2-degenerated Hopf point producing the appearance of a unstable hole inside the feasibility region that was supposed continuously stable. This paper study the effect of using a Flexible AC Transmission System (FACTS) device, named StatCom, on the topological characteristic of the feasibility region. This study is carry out by a multi-parameter bifurcation analysis. The controller is used to damp out Hopf bifurcations, such that the unstable hole inside feasibility region disappears. The study is carried out in a 3-nodes power system, and the controller effect is quantified by comparing the feasibility region geometric topology when the StatCom connected to the system with respect to the results obtained when the controller is not used.**

Index Terms—**Power system stability, Feasibility Region, Bifurcation analysis, FACTS, Power system security.**

I. Introduction

Nowadays, voltage collapse and poorly damping oscillations problems have been of major concerns to engineers in charge of the planning and operation of power systems. Theses instability problems have lead to major disruptions on power systems operation, such as the blackouts taking place in August 1996 WSCC system [1], August 2003 North-East system [2,3], September 2003 Sweden and Italy systems [2,3] and November 2006 Germany to Spain systems [4]. Hence, identification of voltage stability and oscillatory stability boundaries is of great interest for power system dispatchers. Bifurcation theory provides a natural framework for studying the mechanisms associated to these phenomena [5]. Bifurcation theory predicts how the system equilibrium points become instable due to quasi-static changes of system parameters. Depending of the generic model of the power system, two major local bifurcations have been directly related to a monotonic voltage collapse and voltage oscillatory instabilities, namely saddle-node (SN), and Hopf bifurcations, respectively.

The region in the parameter space where all operating points can be reached by continuous variation of parameters without causing instability is called feasibility region [6]. The boundary of this region is composed by bifurcation surfaces since this boundary is related to stability changes on the system equilibrium points. These bifurcation surfaces are determined by different kind of bifurcations. In [6], it was demonstrated that the boundary of a feasibility region associated to locally asymptotically stable equilibrium points was composed by surfaces of saddle node bifurcations, Hopf bifurcations and singularity induced bifurcations. However, degenerate feasibility boundaries were not study. These boundaries arise as those bifurcation surfaces intersect each other, producing an instable region or hole inside the feasibility region. This topological characteristic of the feasibility region was studied in [7] considering the well-known chaotic 3-nodes power system [8]. The study was focused on the feasibility boundary associated to Hopf bifurcations. The importance of this boundary is that once it has been reached, the system will experience either a persistent oscillation or a growing oscillatory transient problem. In this case, the system may lose its stability well before the point of collapse is reached. An extension to this study was presented in [9] by investigating the impact of the exciter voltage limit. It was found that these limits change the feasibility boundary and produce a new hole inside the feasibility region, such that the topological characteristic of this region become even more complicated.

The use of high power electronics based technologies, such as Flexible Alternating Current Transmission Systems (FACTS) and proper controller design, have become essential for the improvement of operation and control of power systems. Owing to their flexibility and fast response, FACTS devices have been used to bifurcation control [10] in order to increase the power system loadability margin [11] as well as to damp out power system oscillations [12]. Hence, it is expected that the use of these kinds of controllers will have an effect on the feasibility region boundaries as well as their topological characteristic.

Based on the afore-mentioned, and recognizing that the knowledge of the proximity of the system's operating point to the feasibility boundary is of great importance to have information about potential emergence of instability problems, the aim of this paper is to study the effect of one of the FACTS controller's family members, named StatCom, on the feasibility region topological characteristic. A 3-nodes power system is considered for this study. The system is represented by a set of differential-algebraic nonlinear equations whose equilibrium points are computed, as two system parameters are varied, in order to obtain the bifurcation surfaces. Based on this analysis, both bifurcation and degenerated bifurcation boundaries are determined with and without the StatCom to assess the controller's effect on the feasibility region topological characteristic. The remainder of the paper is

This work was supported by The National Council of Science and Technology, (CONACyT) , Mexico under grant 194843 .

Héctor R. Carvajal-Pérez is with the Faculty of Electrical Engineering, Universidad de Colima, Colima, México.

Claudio R. Fuerte-Esquivel is with the Faculty of electrical Engineering, Universidad Michoacana de San Nicolás de Hidalgo (UMSNH), Morelia, Michoacan, 58000, Mexico (email:cfuerte@umich.mx).

structured as follows: Section II presents models of the electric components making up the power system to be analyzed. Section III describes theoretical concepts to carry out bifurcation analysis of electric power systems. Section IV discusses the results obtained from the application of multi-parameter bifurcation analysis to find the feasibility region, as well as the effect of the StatCom on the topological structure of this region. Finally, the main results and contributions of this paper are summarized and highlighted in Section V.

II. POWER SYSTEM MODELING

An electric power system can be represented by a set of parameter dependent differential equations constrained by a set of algebraic equations (DAEs), as given by (1).

$$\begin{aligned} \dot{x} &= f(x,y,\beta) \qquad f:\Re^{n+m+p}\to\Re^{n} \\ 0 &= g(x,y,\beta) \qquad g:\Re^{n+m+p}\to\Re^{m} \\ x &\in X\subset\Re^{n} \quad y\in Y\subset\Re^{m} \quad \beta\in \mathrm{B}\subset\Re^{p} \end{aligned} \tag{1}$$

where x is a vector of dynamic state variables, y is a vector of instantaneous state, or algebraic, variables (usually complex node voltages); and β is a set of non-time varying system parameters. Due to the fact that transmission network dynamics are much faster than dynamics of the equipment or loads; it is considered that variables y change instantaneously with variations of the x states. Hence, only the dynamics of the equipment, e.g. generators, controls, FACTS devices, and load at buses, are explicitly modeled by the set of differential equations (1). The set of algebraic equations expresses the mismatch power flow equations at each node. As the power system can be viewed as an interconnection of several electric power plant components, particulars of each model are given below. All variables are given in per unit, unless it is specified otherwise.

A. Generator

In this paper, a two-axis generator model as described in [13] is considered which includes a simple faster exciter loop, a field winding on *d*-axis and a damping winding on *q*-axis.

1) Rotor equations

The rotor mechanical model is given by the swing equations. For the i^{th} generator, these equations are,

$$\begin{aligned} \dot{\delta}_i &= \omega_B s_i \\ \dot{s}_i &= \frac{-D_i s_i + P_{Mi} - P_{gei}}{2H_i} \\ s_i &= \frac{\omega_i - \omega_B}{\omega_B} \end{aligned} \tag{2}$$

where $2H_i$ is the moment of inertia in seconds (sec), D_i is the damping constant, P_{Gei} is the generator's electrical power output, P_{Mi} is the turbine mechanical power injection, δ_i is the generator's rotor angle in radians (rad), ω_B is the synchronous speed in rad/sec, ω_i is the actual rotor speed in rad/sec, and s_i is the generator slip.

The equations of the two electrical systems on the rotor are,

$$\begin{aligned} \dot{E}_q^{'} &= \frac{-E_q^{'} + (x_d - x_d^{'})i_d + E_{fd}}{T_{d0}^{'}} \\ \dot{E}_d^{'} &= \frac{-E_d^{'} - (x_q - x_q^{'})i_q}{T_{q0}^{'}} \end{aligned} \tag{3}$$

where $E_d^{'}$ and $E_q^{'}$ are the transient internal voltage magnitudes on *d* and *q* axis, respectively; x_k and $x_k^{'}$ are the steady state and transient state reactances on axis k=q, d, respectively; $T_{d0}^{'}$ and $T_{q0}^{'}$ are the constant time on *d* and *q* axis, respectively; lastly, E_{fd} is the *DC* controlled voltage field.

2) Stator equations

The following algebraic equations can be obtained by neglecting both stator transients and stator resistance, where the active power generated is measured at terminals.

$$\begin{aligned} E_q^{'} + x_d^{'} i_d &= v_q \\ E_d^{'} - x_q^{'} i_q &= v_d \\ P_{ge} &= E_q^{'} i_q + E_d^{'} i_d + (x_d^{'} - x_q^{'}) i_d i_q \end{aligned} \tag{4}$$

B. Excitation system

The excitation system is considered as shown in Fig. 1, with its equation given by (5).

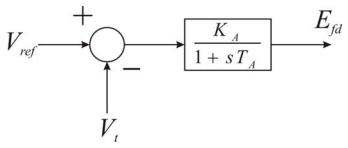

Fig.1. Excitation system.

$$\dot{E}_{fd} = \frac{-E_{fd} + K_A(V_{ref} - V_t)}{T_A} \tag{5}$$

where E_{fd} is the *DC* controlled voltage field, V_{ref} is the reference node voltage, V_t refers to the voltage at the generator terminal, K_A is the control gain and T_A is the excitation system constant time.

C. Network

This model consists of those equations expressing the active and reactive power balances at every *PV* and *PQ* system nodes. For the transmission element connected between nodes *i* and *j*, the active and reactive powers at the i^{th} node are,

$$\begin{aligned} P_{ij} &= V_i^2 G_{ii} + V_i V_j (G_{ij}\cos(\delta_i - \delta_j) + B_{ij} sen(\delta_i - \delta_j)) \\ Q_{ij} &= -V_i^2 B_{ii} + V_i V_j (G_{ij} sen(\delta_i - \delta_j) - B_{ij}\cos(\delta_i - \delta_j)) \end{aligned} \tag{6}$$

Assuming n_g internal generator nodes, n_{PV} *PV* nodes and n_{PQ} *PQ* nodes, V_k and δ_k are the magnitude and phase angle voltages at network nodes, $k = n_g + 1, \ldots, n_g + n_{PV} + n_{PQ}$;

respectively, and $\bar{Y}_{ij} = G_{ij} + jB_{ij}$ is the admittance of the transmission element connected between nodes *i* and *j*.

The mismatch power equations at the network nodes are,

$$\begin{aligned} P_{gei} &= P_{Li} + \sum_{j\in\Omega_i} P_{ij} \qquad \forall i = n_g+1,\ldots,n_g+n_{PV}+n_{PQ} \\ Q_{gei} &= P_{Li} + \sum_{j\in\Omega_i} P_{ij} \qquad \forall i = n_g+n_{PV}+1,\ldots,n_g+n_{PV}+n_{PQ} \end{aligned} \tag{7}$$

where $\Omega_i = \{j : j \neq i\}$ is the set of nodes adjacent to *i*, P_{Li} is the active power demanded by the load embedded at generator terminals and P_{ij} is the active power for the transmission element connected between generator terminals and node *j*.

D. Load.

It is clear that loads rather than generators drive many instability problems, such as voltage collapse. Despite there is not general rule regarding to which load model is reasonable to use, exist an agreement that classical static load models are not adequate to capture load dynamics and study non-linear oscillations [14]. The generic dynamic load model suggested by Dobson [8] based on load voltage dynamics due to Walve [15] is considered in this paper along with a constant power load (P_{1d}, Q_{1d}) in parallel with it. The model for the load embedded at i^{th} bus is given by,

$$\begin{aligned} P_{Li} &= P_{1d} + P_0 + p_1\dot{\delta}_i + p_2\dot{V}_i + p_3 V_i \\ Q_{Li} &= Q_{1d} + Q_0 + q_1\dot{\delta}_i + q_2\dot{V}_i + q_3 V_i^2 \end{aligned} \tag{8}$$

where both sets $\{P_0, Q_0\}$ and $\{p_1, p_2, p_3, q_1, q_2, q_3\}$ are constant powers and fixed values associated to the dynamic load, respectively.

E. StatCom.

One important FACTS component is the StatCom which operates as a shunt connected static var compensator but its capacitive or inductive reactive current is controlled independently of the *ac* system voltage by using a three phase voltage source converter (VSC). The mathematical model adopted in this paper is that reported in [16]. An equivalent circuit for the StatCom is shown in Fig. 2, where V_{abc} are the system-side phase voltages, R_s and L_s represent the transformer parameters and E_{abc} are the VSC *ac* side phase voltages given by,

$$E_a = kV_{dc}\cos(\omega_B t + \alpha) \tag{9}$$

where V_{dc} is the voltage across the *dc* capacitor, *k* is the modulation gain that relates the *dc* voltage to the peak voltage on the *ac* side, and α is the phase angle of the injected voltage.

Based on the StatCom equivalent circuit, the set of ordinary differential equations in the *dq* frame of reference is,

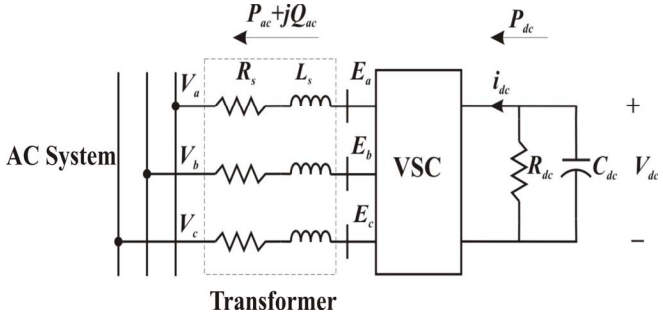

Fig. 2. Equivalent circuit of the StatCom.

$$\begin{aligned} \frac{d}{dt}i_d &= -\frac{R_s\omega_B}{L_s}i_d + (s_i\omega_B + \omega_B)i_q + \frac{k\omega_B}{L_s}\cos(\alpha+\delta_i)V_{dc} - \frac{V_i}{L_s}\cos\delta_i \\ \frac{d}{dt}i_q &= -\frac{R_s}{L_s}i_q - (s_i\omega_B + \omega_B)i_d + \frac{k}{L_s}sin(\alpha+\delta_i)V_{dc} - \frac{V_i}{L_s}sin\delta_i \\ \frac{d}{dt}V_{dc} &= \left(\frac{1}{C_{dc}}\right)\left(-k\cos(\alpha+\delta_i)i_d - ksin(\alpha+\delta_i)i_q - \frac{V_{dc}}{R_{dc}}\right) \end{aligned} \tag{10}$$

where i_d and i_q are the injected *dq* StatCom currents, R_{dc} represents the switching losses and $V_i\angle\delta_i$ is the RMS system-side voltage at the StatCom bus.

The algebraic equations representing the power flow balance at the StatCom bus are given by (11), where $Y_{ij}\angle\phi_{ij}$ is the (*i*,*j*)th element of the admittance matrix.

$$\begin{aligned} 0 &= V_i(i_d\cos\delta_i + i_q sin\delta_i) - V_i\sum_{j=1+n_g}^{n_g+n_{PV}+n_{PQ}} V_j Y_{ij}\cos(\delta_i - \delta_j - \phi_{ij}) \\ 0 &= V_i(i_d sin\delta_i - i_q\cos\delta_i) - V_i\sum_{j=1+n_g}^{n_g+n_{PV}+n_{PQ}} V_j Y_{ij} sin(\delta_i - \delta_j - \phi_{ij}) \end{aligned} \tag{11}$$

A Proportional-Integral control is used to adjust the voltage response of the StatCom. The block diagram of the control is shown in Fig. 3, where V_{dc}^* and Q_{ac}^* are reference quantities related to the voltage across the *dc* capacitor and the reactive power injected by the controller, respectively.

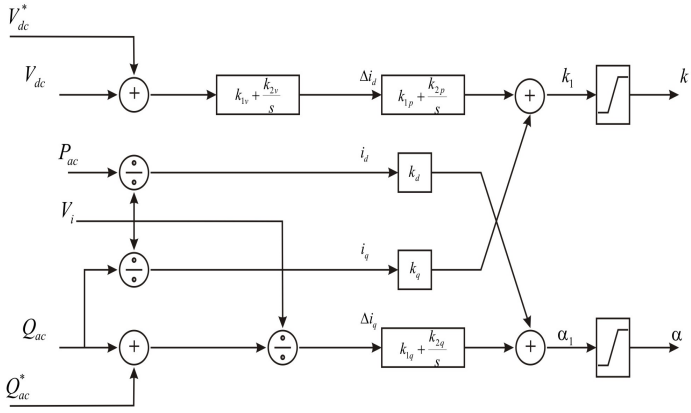

Fig. 3. PI-based control for the StatCom.

The set of DAE control equations is obtained assuming a decoupled control approach, i.e. $K_d = K_q = 0$,

$$\begin{aligned}\dot{x}_1 &= k_{2v}\left(V_{dc}^{*}-V_{dc}\right)\\ \dot{x}_2 &= k_{2p}\Delta i_d\\ \dot{x}_3 &= k_{2q}\left(\frac{Q_{ac}-Q_{ac}^{*}}{V}\right)\end{aligned} \tag{12}$$

$$\begin{aligned}\Delta i_d &= k_{1v}\left(V_{dc}^{*}-V_{dc}\right)+x_1\\ \alpha_1 &= k_{1q}\left(\frac{Q_{ac}-Q_{ac}^{*}}{V}\right)+x_3\\ k_1 &= k_{1p}\Delta i_d + x_2\end{aligned} \tag{13}$$

The control limits are represented as,

$$\begin{aligned}k &= k_{\lim}\tanh\left(\frac{k_1}{k_{\lim}}\right)\\ \alpha &= alfa_{\lim}\tanh\left(\frac{\alpha_1}{alfa_{\lim}}\right)\end{aligned} \tag{14}$$

III. Bifurcation Analysis

Bifurcation analysis is related to the emergence of sudden changes in a power system response arising from smooth, continuous variations on system parameters. These changes, or bifurcations, can be obtained by the small-signal stability analysis of the power system equilibrium points, as described below.

A. Equilibrium Solutions and Stability Analysis

Equilibrium analysis is the first step to determine local stability and bifurcations of the power system near an equilibrium point. For an arbitrary fixed set of parameters β_e, a power system equilibrium point is computing by solving the set of nonlinear algebraic equations given by,

$$\begin{aligned}0 &= f(x,y,\beta_e)\\ 0 &= g(x,y,\beta_e)\end{aligned} \tag{15}$$

The set of equilibrium points defined by (16) characterizes a *p*-dimensional equilibrium manifold in the state space of X, Y; and indicates that the system is at rest, but it does not imply stability.

$$EQ=\{(x,y,\beta)\in X \text{ x } Y \text{ x } \mathrm{B} : f(x,y,\beta)=0,\ g(x,y,\beta)=0\} \tag{16}$$

The small-signal stability of an isolated equilibrium point E_p can be determined by linearising (1) around E_p and carrying out an eigenvalue analysis of the resulting system given by,

$$\begin{bmatrix}\Delta\dot{x}\\ 0\end{bmatrix}=\left[\begin{array}{cc}\frac{\partial f}{\partial x} & \frac{\partial f}{\partial y}\\ \frac{\partial g}{\partial x} & \frac{\partial g}{\partial y}\end{array}\right]_{E_p}\begin{bmatrix}\Delta x\\ \Delta y\end{bmatrix} \tag{17}$$

Since the eigenvalues are functions of the system parameters β_e and the eigenvalues locations determine the stability of the DAEs, the parameters determine the stability properties of (1).

B. ODE equivalent system

The stability theory of nonlinear dynamical systems described by ordinary differential equations (ODEs) is very well developed [5] and can be applied to assess the stability properties of a DAE system's equilibrium point. Based on the implicit function theorem and Schur's theorem [5,14], it is possible to establish conditions under which an ODE equivalent system of (1) can be derived with the same dynamic and algebraic properties as the full model.

Equations $g(x,y,\beta)=0$ can be used to solve for the fast variables y in terms of slow dynamic variables x and then substitute this solution into $f(x,y,\beta)=0$ to obtain an equivalent set of ODEs. However, it is not trivial to get this reduced model due to the large number of variables and the nonlinear nature of $g(x,y,\beta)$. In principle, however, this reduction can be achieved locally by using the implicit function theorem which affirm that there exists a function $\psi(x,\beta)$ defined in the neighborhood of the equilibrium point with $y_0=\psi(x_0,\beta_0)$, such that $y=\psi(x,\beta)$ and satisfies $g\left(x,\psi(x,\beta),\beta\right)=0$ [5]. It follows that an equivalent set of ODEs given by (18) could represent locally the dynamics of the DAE model (1) as well as its stability properties.

$$\dot{x}=f_e\left(x,\psi(x,\beta),\beta\right) \tag{18}$$

A necessary condition to ensure the validity of such a system reduction is that the equilibrium point is away from the singular set

$$S_s=\left\{(x,y,\beta)\in X \text{ x } Y \text{ x } \mathrm{B} : \det\left(\left.\frac{\partial g(x,y,\beta)}{\partial y}\right|_{E_p}\right)=0\right\} \tag{19}$$

Hence, for an $E_p\notin S_s$, the linearised equivalent ODE model is obtained from Schur's theorem and it is given by,

$$\Delta\dot{x}=\left[\frac{\partial f(\cdot)}{\partial x}-\frac{\partial f(\cdot)}{\partial y}\left(\frac{\partial g(\cdot)}{\partial y}\right)^{-1}\frac{\partial g(\cdot)}{\partial x}\right]_{E_p}\Delta x=J_{RS}\big|_{E_p}\,\Delta x \tag{20}$$

According to the Lyapunov stability theory [5], the equilibrium point E_p is stable if all eigenvalues of $J_{RS}\big|_{E_p}$ have negative real parts. Furthermore, these eigenvalues can indicate us the appearance of two types of codimension-1 (single parameter) generic local bifurcations, namely SNB and HB [5].

C. Saddle Node Bifurcations (SNB)

The SNB arises when a stable equilibrium point E_{PS} coalesces with a nearby unstable equilibrium point E_{PU} and disappears, causing the system to loose stability. Formally, the system (18) undergoes the SNB at the single bifurcation parameter $\beta_B=\beta_0$ and equilibrium point E_p when the following conditions are satisfied;

1. $J_{RS}\big|_{E_p}$ has exactly one eigenvalue with a positive real part and the rest of eigenvalues have negative real parts, with right eigenvector υ and left eigenvector w.

2. $w^t \left.\dfrac{\partial f_e(\cdot)}{\partial \beta_B}\right|_{E_p} \neq 0$

3. $w^t \left.\dfrac{\partial^2 f_e(\cdot)}{\partial^2 \beta_B}\right|_{E_p} \upsilon\upsilon \neq 0$

The first condition implies that the Jacobian matrix is singular; the second and third conditions ensure transversatility so that the bifurcations are not degenerate cases. Depending on the sign of the expressions in conditions 2 and 3, there are no equilibria near E_p when the bifurcation parameter is $\beta_B < \beta_0$ $(\beta_B > \beta_0)$ and two equilibria near E_p for each bifurcation parameter value $\beta_B > \beta_0$ $(\beta_B < \beta_0)$.

D. Hopf Bifurcations (HB)

When a complex conjugate pair of eigenvalues of $J_{RS}\big|_{E_p}$ crosses the imaginary axis and moves into the right-half plane, the system may star oscillating, such that a Hopf bifurcation has taken place. Formally, the system (18) undergoes the HB at the single bifurcation parameter $\beta_B = \beta_0$ and equilibrium point E_p when the following conditions are satisfied;

1. The Jacobian matrix $J_{RS}\big|_{E_p}$ has a simple pair of pure imaginary eigenvalues $\gamma(\beta_0) = \pm j\varpi(\beta_0)$ while all other eigenvalues have nonzero real parts.

2. $\left.\dfrac{d\{\mathrm{R_e}\gamma(\beta_B)\}}{d\beta_B}\right|_{\beta_0} \neq 0$

The first condition ensures that E_p is a nonhyperbolic point whilst the second condition implies a transversal or nonzero speed crossing of the imaginary axis [5].

E. Computation of the feasibility region

Owing to the multi-parameter variation existing in power systems, it is necessary to carry out a multi-parameter bifurcation study to obtain the system's feasibility region. The procedure adopted in this paper to carry out this study is based on a series of one-parameter bifurcation analysis. This analysis consists of solving the set of differential-algebraic equations representing the power system as one of the system parameters is varied while all the other parameters are held constant. It implies to solve n equations in n+1 unknowns, such that solutions will be curves rather than points. An approach to determine these solutions is to generate successive equilibrium points along the curve based on the principle of continuation [5]. The representation of this solution curve in the state-parameter space is referred to as one-parameter bifurcation diagram. A series of this sort of bifurcation diagrams are obtained by repeating the described process for different fixed values of the parameters held constant. Hence, surfaces of stability regions can be constructed by putting together a series of one-parameter bifurcation diagrams. These diagrams are obtained by using the popular continuation-based program named XPP-AUTO [17].

IV. Study Cases

This section presents numerical results of a multi-parameter bifurcation analysis of the 3-bus system shown in Fig. 4. This system has been employed by several researches to illustrate ideas regarding to dynamic instabilities and growing oscillations observed in real power systems due to voltage collapse phenomenon. Although the analysis is applied on the theoretical model of this simple power system, it is also valid for realistic power systems. The 3-bus system may be viewed as an equivalent circuit for a local area of interest connected to a large network. The large network is modeled as an infinite bus represented by a voltage source providing constant voltage $E_b\angle 0$ regardless of the value of system parameters. The generator terminal voltage is $V_t\angle\delta_m$ whilst transmission line admittances are given by $Y_1\angle\phi_1$ and $Y_2\angle\phi_2$. Lastly, the load voltage is $V_L\angle\delta_L$. The generator is modeled by equations (2)-(4) neglecting the damper winding. The excitation system is modeled by (5). The load consists of a constant *PQ* load in parallel with an induction motor which is modeled by (8). A multi-parameter bifurcation diagram of the voltage magnitude at the load bus is obtained with and without the StatCom embedded in the system by varying the exciter amplifier time constant and the generator's input mechanical power, $p = [T_A, P_m]^T \in \Re^2$.

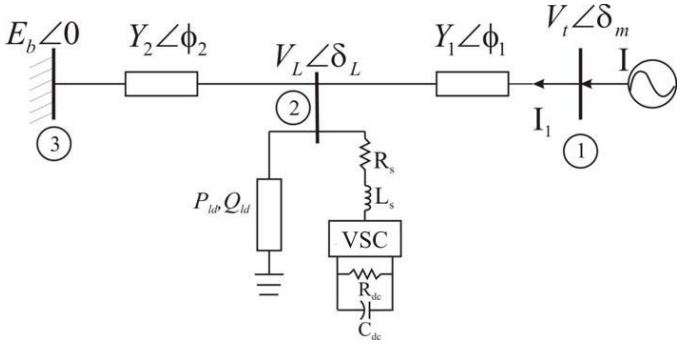

Fig. 4. Three bus system.

A. Feasibility region without StatCom

This section presents the study to obtain the feasibility region when the StatCom is not connected in the system. Owing to the system's size, it is possible to solve for the algebraic variables $y = [P_{ge}, I_d, I_q, E_d^{'}, V_t, V_d, V_q, P, Q]^T \in \Re^9$ in terms of the state variables $x = [\delta_m, s_m, E_q^{'}, E_{fd}, \delta_L, V_L]^T \in \Re^6$ to obtain the system of purely ordinary differential equations (18) given by,

$$\dot{\delta}_m = \omega_B s_m \tag{21}$$

$$\dot{s}_m = \frac{-Ds_m + P_m - \left(E_q^{'} i_q + E_d^{'} i_d + (x_d^{'} - x_q^{'}) i_d i_q\right)}{2H} \tag{22}$$

$$\dot{E}_q^{'} = \frac{-E_q^{'} + (x_d - x_d^{'}) I_d + E_{fd}}{T_{d0}^{'}} \tag{23}$$

$$\dot{E}_{fd} = \frac{-E_{fd} + K_A (V_{ref} - V_t)}{T_A} \tag{24}$$

$$\dot{\delta}_L = \frac{Q - Q_{1d} - Q_0 - q_2 V_L - \left(q_3 - B_c\right) V_L^2}{q_1} \tag{25}$$

$$\dot{V}_L = \frac{P - P_{1d} - P_0 - \frac{p_1}{q_1}\left(Q - Q_{1d} - Q_0 - q_2 V_L - (q_3 - B_c) V_L^2\right) - p_3 V_L}{p_2} \tag{26}$$

The active and reactive powers terms P and Q given in equations (25) and (26) are computed by (27) and (28), respectively, where $\theta_1 = \delta_L - \delta_m - \phi_1$ and $\theta_2 = \delta_L - \phi_2$. These powers correspond to the power supplied to the load from the network. System parameters are given as indicate in Table I.

$$\begin{aligned} P = {} & V_t V_L Y_1 \cos(\theta_1) - V_L^2 Y_1 \cos(\phi_1) \\ & + E_b V_L Y_2 \cos(\theta_2) - V_L^2 Y_2 \cos(\phi_2) \end{aligned} \tag{27}$$

$$\begin{aligned} Q = {} & V_t V_L Y_1 sin(\theta_1) + V_L^2 Y_1 sin(\phi_1) \\ & + E_b V_L Y_2 sin(\theta_2) + V_L^2 Y_2 sin(\phi_2) \end{aligned} \tag{28}$$

TABLE I. SYSTEM DATA

variable	value	variable	value	parameter	value
Y_1	4.9752 pu	E_b	1 pu	p_1	0.24 pu
ϕ_1	-1.4711 rad	E_m	1 pu	q_1	-0.02 pu
Y_2	1.6584 pu	H	2.894 seg	p_2	1.7 pu
ϕ_2	-1.4711 rad	ω_B	377 rad/seg	q_2	-1.866 pu
x_d	1.79 pu	D	0.05 pu	p_3	0.2 pu
x_q	1.71 pu	P_0	0.4 pu	q_3	1.6 pu
x'_d	0.169 pu	Q_0	0.8 pu	B_c	0.2 pu
x'_q	0.23 pu	P_{1d}	0.0 pu	K_A	200
T'_{d0}	4.3 seg	Q_{1d}	0.0 pu	V_{ref}	1.122 pu

The single-parameter bifurcation diagram of the voltage magnitude at the load bus, considering P_m as a bifurcation parameter, is shown in Fig. 5. This diagram is obtained based on the following initial conditions, V_L = 1.012 pu, δ_L = 0.1312 rad, δ_m = 0.8684 rad, ω = 0 rad/sec, E_q = 1.0556 pu , E_{fd} = 2.3684 pu, T_A = 0.05 and P_m = 0.4 pu. The solid and broken lines indicate stable and unstable stationary trajectories. An unstable/subcritical Hopf bifurcation (UHB_1) point is detected at P_m = 0.6086 pu. Stable/supercritical bifurcation points are detected at values of P_m = 1.1558 pu (SHB_1) and P_m = 1.1912 pu (SHB_2). When P_m is increased until 1.9607, a zero eigenvalue appears such that emerge a saddle node bifurcation point (SNB).

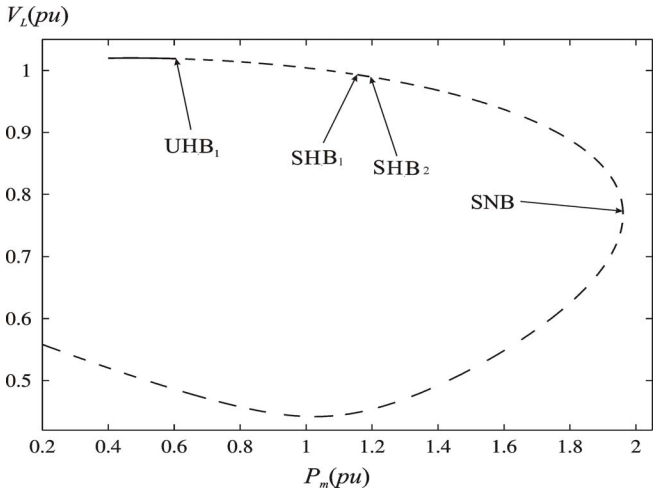

Fig. 5. Single-parameter bifurcation diagram without StatCom.

The multi-parameter bifurcation diagram of the voltage magnitude at the load bus is shown in Fig. 6. The feasibility region defined by the set of all operating points which can be reached quasi-statically from a given operating point without driving any of the eigenvalues to the instability on the complex plane corresponds to the bright-grey area. As demonstrated in [6], this region is bounded by curves composed by connected equilibrium points related to the same type of bifurcation. In this case, there are three curves denoted as HB_1, HB_2 and HB_3 which correspond to a supercritical (UHB_1), subcritical (SHB_1) and subcritical (SHB_2) Hopf bifurcation, respectively. Owing to the fact that HB_1 and HB_2 curves coalesce at points M and N, as shown in Fig. 7, exists a hole (instability region) inside the feasibility region. This hole takes place due to the critical eigenvalues do not cross the imaginary axis but they are tangent to this axis, such that the transversal condition is violated [18,19]. Hence, a 2-degenerated Hopf bifurcation point appear due to bifurcations points H_1 and H_2 coalesce at points M and N [18,19]. A detailed analysis of the occurrence of this hole is given in [20].

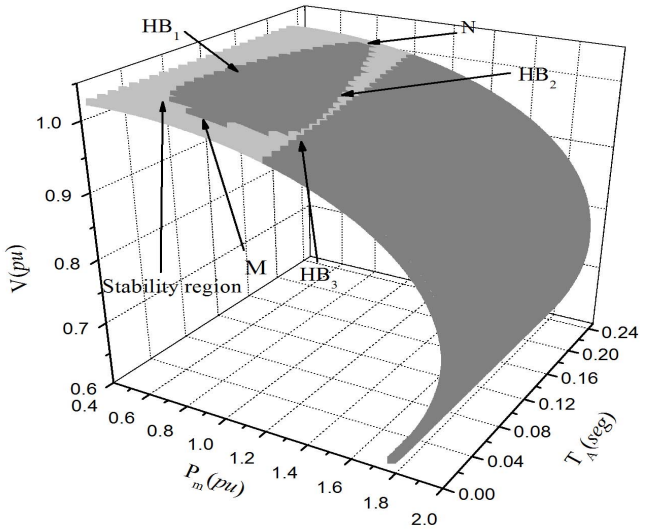

Fig. 6. Multi-parameter bifurcation diagram without StatCom.

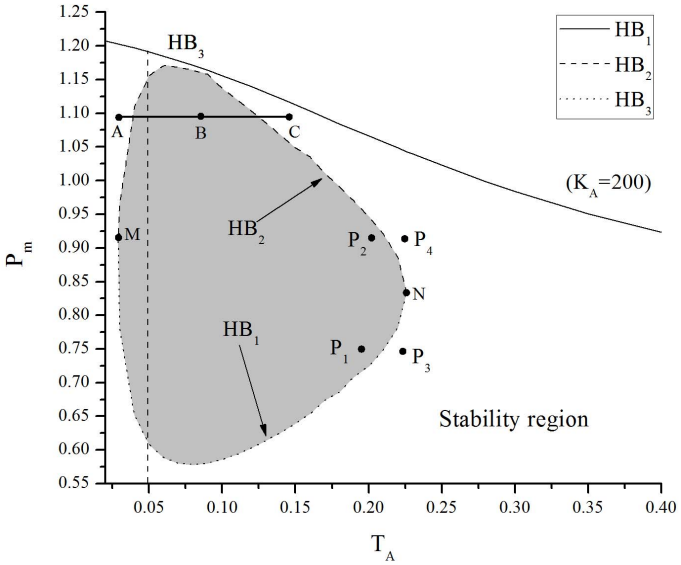

Fig. 7. Hole in the feasibility region without StatCom.

B. *Feasibility region with StatCom*

The StatCom effect on the feasibility region topology is presented in this section. For this purpose, the controller is connected at load bus as indicated in Fig. 4. The StatCom parameters have been selected as given in Table II [21].

TABLE II. STATCOM DATA

variable	value	variable	value	variable	value
R_s	0.01 pu	K_{1p}	0.1	K_{2p}	-0.05
L_s	0.1 pu	K_{1v}	3	K_{2v}	0.5
C	0.7 pu	K_{1q}	0.3	K_{2q}	0.15
R_{dc}	22 pu	$K_{\lim}$	1	$AlI_{\lim}$	1 pu
V_{dc}^*	1.951 pu	Q_{ac}^*	0.2 pu		

The state variables vector is given by (29), whilst the algebraic variables vector is given by (30). The set of equations (12) are added to (21)-(26) to include the StatCom in the mathematical formulation. Furthermore, the power flow balance equations are modified as given by (31) and (32), where the last term in both equations corresponds to the power exchanged between the controller and the power system.

$$x = [\delta, s_m, E_q^{'}, E_{fd}, \delta_L, V_L, I_{d1}, I_{q1}, V_{dc}, x_1, x_2, x_3]^T \in R^{12} \quad (29)$$

$$y = [P_g, I_d, I_q, E_d^{'}, V_t, v_d, v_q, P, Q, \Delta I_{d1}, k_1, \alpha_1]^T \in R^{12} \quad (30)$$

$$\begin{aligned} P = {} & V_t V_L Y_1 \cos(\theta_1) - V_L^2 Y_1 \cos(\phi_1) \\ & + E_b V_L Y_2 \cos(\theta_2) - V_L^2 Y_2 \cos(\phi_2) \\ & + V_L (I_{d1} Cos\delta_L + I_{q1} Sin\delta_L) \end{aligned} \quad (31)$$

$$\begin{aligned} Q = {} & V_t V_L Y_1 sin(\theta_1) + V_L^2 Y_1 sin(\phi_1) \\ & + E_b V_L Y_2 sin(\theta_2) + V_L^2 Y_2 sin(\phi_2) \\ & + V_L (I_{d1} sin\delta_L - I_{q1} cos\delta_L) \end{aligned} \quad (32)$$

The following initial conditions are considered to obtain a stable equilibrium point which is used to compute the single-parameter bifurcation diagram shown in Fig. 8; V_L = 1.012 pu, δ_L = 0.1312 rad, δ_m = 0.8684 rad, ω = 0 rad/sec, E'_q = 1.0556 pu , E_{fd} = 2.3684 pu, T_A = 0.05, P_m = 0.4 pu, I_{d1} = -0.21302 pu, I_{q1} = -0.1521 pu, V_{dc} = 1.95 pu, x_1 = 0 pu, x_2 = 0.5734 pu, and x_3 = -0.001955 pu.

From the bifurcation diagram it is observed that two bifurcations are only detected. The bifurcation points SHB and SNB take place at values of P_m = 1.4131 pu and P_m = 2.1418 pu, respectively. Hence, the reactive power injected by the StatCom, $Q_{ac}^* = 0.2$ pu, increased the loadability of the system. On the other hand, the controller helped to damp out the oscillations associated to one subcritical Hopf bifurcation and one supercritical Hopf bifurcation. The removal of these two bifurcations produces the elimination of the hole inside the feasibility region. It is demonstrated by the multi-parameter bifurcation diagram shown in Fig. 9.

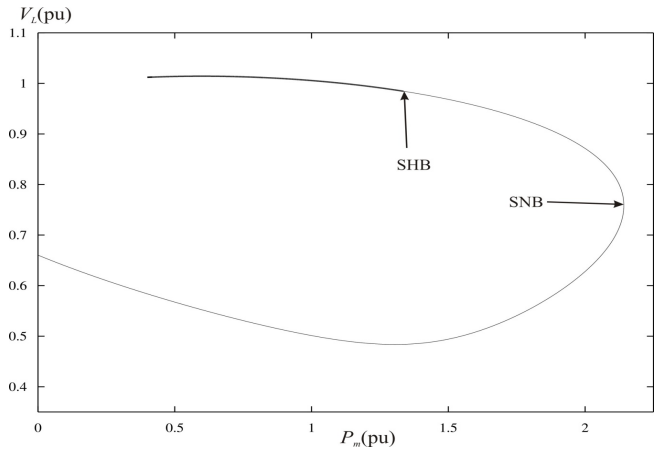

Fig. 8. Single-parameter bifurcation diagram with StatCom.

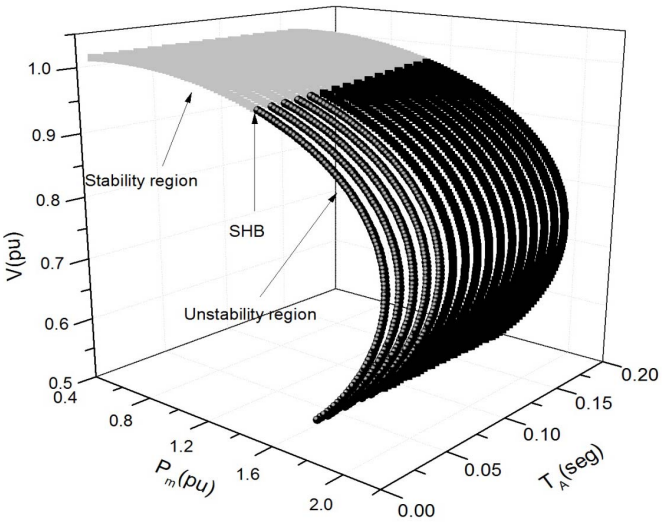

Fig. 9. Multi-parameter bifurcation diagram with StatCom.

V. CONCLUSIONS

Bifurcation theory has been applied to study topological characteristics of the feasibility region of a 3-nodes power system as well as changes on its structural stability. Based on a multi-parameter bifurcation analysis, through numerical simulations, it has been demonstrated that the boundary of this feasibility region is composed by bifurcation surfaces. It has

been also demonstrated the occurrence of an unstable hole inside the feasibility region that was supposed continually stable. The appearance of this hole takes place due to the emergence of a 2-degenerated Hopf point. A system will experience dynamically unstable oscillations if it is operating inside this hole, and may face serious problems from an operation viewpoint, such as voltage instabilities. In order to avoid these problems, a Flexible AC Transmission System (FACTS) device, named StatCom, has been employed for controlling the occurrence of Hopf bifurcations and for increasing the system's loadability conditions. The application of this controller is suitable to damp out Hopf bifurcations and eliminate the appearance of an unstable hole, such that a unbroken feasibility region can be obtained. Despite the study has been conducted in a small power system, the observations are quite general and may form a useful basis for the analysis of more complex and large systems.

REFERENCES

[1] Kosterev D.N., Taylor C.W. and Mittelstadt W.A., "Model validation for the August 10, 1996 WSCC system outage," IEEE *Trans. on Power Syst*., Vol. 14, No. 3, pp. 967-979, Aug. 1999.

[2] Bialek J.W., "Recent blackouts in US, Canada and Continental Europe: is liberalisation to Blame?," *Ninth POWER Research Conference on Electricity Restructuring*, University of California, Berkeley, March 2004, http://www.see.ed.ac.uk/~jbialek/publications.html.

[3] Andersson G., Donalek P., Farmer R., Hatziargyriou N., Kamwa I., Kundur P., Martins N., Paserba J., Pourbeik P., Sanchez-Gasca J., Schulz R., Stankovic A., Taylor C., and Vittal V., "Causes of the 2003 major grid blackouts in North America and Europe, and recommended means to improve system dynamic performance," IEEE *Trans. on Power Syst.*, Vol. 4, No. 4, pp. 1922-1928, Nov. 2005.

[4] Keats K. and McCarthy C., "Recent blackouts support the need for increased European coordination," ICF International, 5 pages, 2006, Available from http://www.icfi.com/Markets/Energy/doc_files/europe-blackout-2006.pdf.

[5] Kuznetsov Y. A., *Elements of Applied Bifurcation Theory*, Second Edition, Springer-Verlag, 1998.

[6] Venkatasubramanian V., Schättler H. and Zaborszky J., "Local bifurcations and feasibility regions in differential-algebraic systems," IEEE *Trans. on Automatic Control*, Vol. 40, No. 12, pp.1992-2013, Dec. 1995.

[7] Jia H., Yu X. and Zhang P., "Topological characteristic studies on power system small signal stability region," IEEE Power Engineering Society General Meeting, 18-22 June 2006, 7 pages.

[8] Dobson I., Chiang H.D. and Thorp J.S., "A model of voltage collapse in electric power systems," *IEEE Proc. of 27th Conference on Decision and Control*, Austin Texas, Dec. 1988, pp.2104-2109.

[9] Yu X., Cao S., Jia H. and Zhang P., "Impact of the exciter voltage limit to power system small signal stability region," *IEEE Power Engineering Society General Meeting*, 24-28 June 2007, 7 pages.

[10] Srivastava K.N. and Srivastava S.C., "Elimination of dynamic bifurcation and chaos in power systems using FACTS devices," IEEE *Trans. on Circ. and Syst.*-I, Vol. 45, No. 1, pp. 72-78, Jan. 1998.

[11] Canizares C.A. and Faur Z.T., "Analysis of SVC and TCSC controllers in voltage collapse," IEEE *Trans. on Power Syst*., Vol. 14, No. 1, pp. 158-165, Feb. 1999.

[12] Mithulananthan N., Canizares C.A., Reeve, J. and Rogers G.J., "Comparison of PSS, SVC, and STATCOM controllers for damping power system oscillations," IEEE *Trans. on Power Syst*., Vol. 18, No. 2, pp. 786-792, May 2003.

[13] Rajesh K.G. and Padiyar K.R, "Bifurcation analysis of a three node power system with detailed models," *International Journal of Electrical Power and Energy Systems*, Vol. 21, pp.375-393, Nov. 1999.

[14] Van Cutsem T., Vournas C., *Voltage Stability of Electric Power Systems*, Kluwer Academic Publishers, 1998.

[15] Walve K., "Modeling of power system components at severe disturbances", CIGRÉ paper 38-18, International conference on large high voltage electric systems, August 1986.

[16] Dong L., Crow M. L., Yang Z., Shen C., Zhang L. and Atcitty S., "A Reconfigurable FACTS System for University Laboratories," IEEE *Trans. on Power Syst*., Vol. 19, No. 1 pp. 120-128, February 2004.

[17] Ermentrout B., *Simulating, Analyzing and Animating Dynamical Systems: A Guide to XPPAUT for Researchers and Students*, SIAM 2002.

[18] Golubitsky M. and Langford W. F., "Classification and unfoldings of degenerate Hopf bifurcations," *J. Differential Equations*, Vol. 41, No. 3, pp. 375-415, 1981.

[19] Moiola J. L. and Chen G., *Hopf Bifurcation Analysis: A Frequency Domain Approach*, World Scientific Publishing Co. 1996.

[20] Jia H., Yu X. and Zhang P., "Topological Characteristic Studies on Power System Small Signal Stability Region". *IEEE Power Engineering Society General Meeting,* 2006, 7 pages.

[21] Lenh P., "Exact modeling of the voltage source converter," *IEEE Trans. Power Delivery*, Vol. 17, No. 1, pp. 217-222, January 2002.

Héctor R. Carvajal-Pérez received the B.Eng. (Hons.) degree in 1999 from the University of Colima, Colima, México, and the MS degree in 2007 from the Universidad Michoacana de San Nicolás de Hidalgo (UMSNH), Morelia, México, in 2004. He is currently a Lecturer at the Universidad de Colima.

Claudio R. Fuerte-Esquivel (M'91) received the B.Eng. (Hons.) degree from the Instituto Tecnológico de Morelia, Morelia, México, in 1990, the MS degree (*summa cum laude*) from the Instituto Politécnico Nacional, México, in 1993, and the PhD degree from the University of Glasgow, Glasgow, Scotland, U.K., in 1997. Currently, he is an Associate Professor at the Universidad Michoacana de San Nicolás de Hidalgo (UMSNH), Morelia, where his research interests lie in the dynamic and steady-state analysis of FACTS.